A HIGHER-ORDER NUMERICAL SCHEME FOR SHALLOW WATER MAGNETO-HYDRODYNAMICS EQUATIONS

SIDRAH AHMED

Sukkur IBA University
E-mail: dr.sidrah@iba-suk.edu.pk

Abstract - This work presents fourth-order conservation element solution element method for one-dimensional shallow water magnetohydrodynamics model. The method is based on unified treatment of spatial and temporal dimensions contrary to finite difference and finite volume method. Moreover the schemes is developed using the conservative formulation and do not require change in source term for treating the degenerate hyperbolic nature of shallow water magnetohydrodynamics system. The accuracy and robustness of extended method is tested by applying to benchmark test from the literature.

I. INTRODUCTION

Gilman was the pioneer to introduce the shallow water magnetohydrodynamics (hereafter referred as SWMHD) system to mathematically model the physical phenomena in the solar tachocline [7]. The solar tachocline is a thin region inside a star where heat radiates from the interior zone to the outer outer turbulent zone predominantly. Its thickness ranges between 2 to 5 percentage of the solar radius. Because of predominantly radiative heat transfer and its thin vertical thickness the tachocline can be described similarly to ocean and atmosphere. This urges the introduction of MHD analogue of shallow water system (SW) to study physical processes in solar tachocline. Although the SWMHD system has been build upon one layer assumption, it is possible to add little changes to link more than one layer as in hydrodynamics case [Ripa]. This indeed allows to study several kind of solar dynamics within solar tachocline reference their in [3], [4], [5], [7].

Following the derivations by [7] and Rossmanith [13], the SWMHD system is written below for incompressible flow under magnetohydrodtatic equilibrium in the z-direction.

$$\frac{\partial}{\partial z}\left(p+\frac{\|\boldsymbol{B}\|^2}{2}\right)=\rho g, \tag{1}$$

$$p+\frac{\|\boldsymbol{B}\|^2}{2}=\rho g z, \tag{2}$$

$$\int_0^h\left(p+\frac{\|\boldsymbol{B}\|^2}{2}\right)dz=\rho g\frac{h^2}{2} \tag{3}$$

$$\rho \equiv \text{constant}, \tag{4}$$

Combining the divergence constraint $\nabla\cdot(hB)$ to above and considering only one dimension give the one dimensional SWMHD equations in the conservative formulation below as:

$$\frac{\partial u}{\partial t}+\frac{\partial f}{\partial x}=\begin{bmatrix}h\\ hv_1\\ hv_2\\ hB_1\\ hB_2\end{bmatrix}_t+\begin{bmatrix}hv_1\\ hv_1^2+\frac{1}{2}gh^2-hB_1^2\\ hv_2^2+\frac{1}{2}gh^2-hB_2^2\\ hv_1v_2-hB_1B_2\\ hv_1B_2-hv_2B_1\end{bmatrix}_x=\begin{bmatrix}0\\0\\0\\0\\0\end{bmatrix} \tag{5}$$

$$\frac{\partial(hB_1)}{\partial x}=0, \tag{6}$$

where g is the gravitational constant, the variables v_1,v_2,B_1,B_2 are the velocity and magnetic field components respectively and h is the layer depth. This system is degenerate hyperbolic due to the last equation $\nabla\cdot(hB) = 0$. Hence in order to develop a Riemann solver for numerical solution of SWMHD model one must needs to relax the equation $\nabla \cdot (hB) = 0$. This will need an addition of extra source term as can be seen in [17]. This is one of the reasons to present my work based on developing a numerical scheme without change in source term.

The one and two dimensional SWMHD system has been solved numerically with different schemes [9], [12], [13], [14]. Due to the eigenvalue structure of MHD analogue of shallow water system, it is obvious to design a robust and accurate numerical method particularly for one dimensional case to obtain a higher order extension that capture all waves region. This is the second reason to carry out the present work. The aim of this paper is to build a novel method for one dimensional SWMHD model which possess following features:

a. The method should be accurate for one dimensional case
b. It is easy to extend the method to higher dimensions
c. There is no need of Riemann solvers
d. There is no need to change the source term. The present work follows [18] , in which authors have presented a fourth order CESE method for MHD system. CESE method is widely applied to solve Riemann problems associated to hyperbolic conservation laws. It was first proposed by Chang et al [2]. Now a large number of studies are available in the literature that demonstrate the CESE method's robustness, easy implementation process and accuracy [8], [9], [10], [11], [12], [15], [18]. This paper is organized in four section. The ongoing section gives an introduction of SWMHD model and the numerical schemes that have been applied to this system. I have tried to emphasize on the causes that urges to develop a higher order CESE scheme for this model. The second section

comprises of detailed formulation of fourth order CESE scheme for one dimensional SWMHD equations. Third section includes the numerical test case that demonstrate the reliability of present work. At the end, concluding remarks are given about this work and some future extensions.

II. FOURTH-ORDER CESE SCHEME

The fourth-order CESE scheme is based on the same basic concept of the second-order CESE scheme in [19]. Let us consider the space-time Cartesian coordinates system $E_2(x,t)$, where x is the spatial coordinate combined with the time coordinate t. Eq.5 can be rewritten as

$$\nabla \cdot h_m = 0, \qquad (7)$$

where $h_m = (f_m,u_m)$,(m = 1,· · ·,5) is the spacetime flux vector and$\nabla = (\frac{\partial}{\partial x}, \frac{\partial}{\partial t})$. Integrating 5 over the arbitrary control volume V and applying the Gausss divergence theorem in the 2D spacetime domain $E_2(x,t)$, allows to write the following form:

$$\int_{A(V)} h_m \cdot ds = 0, \qquad (8)$$

A(V) where A(V) denotes the closed boundary of any spacetime region V in $E_2(x,t)$, da = (dδ)n, with the area dδ and the unit outward normal vector n. Moreover h_m ·ds denotes the total spacetime flux leaving the surface element da.

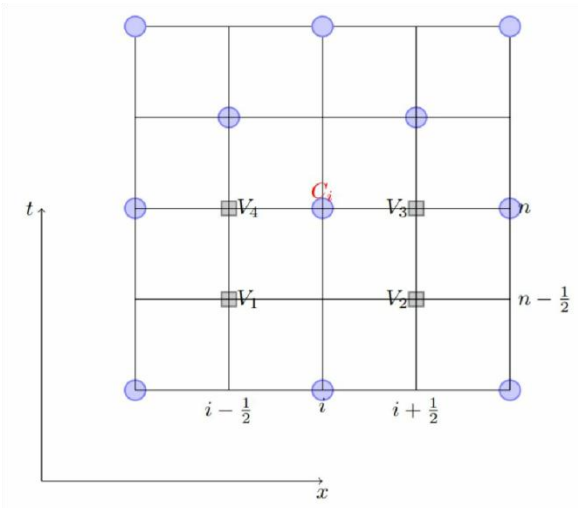


Fig. 1: Space-time discretized grid.

Figure 1 shows the staggered mesh discretization of spacetime domain in Cartesian coordinates. Each node represented by a dot is associated with a conservation element and solution element. Solution is stored at nodes. The staggered mesh ensures that the solution is stored uniquely at each node.
As an example consider the point C_i as an example. Figure

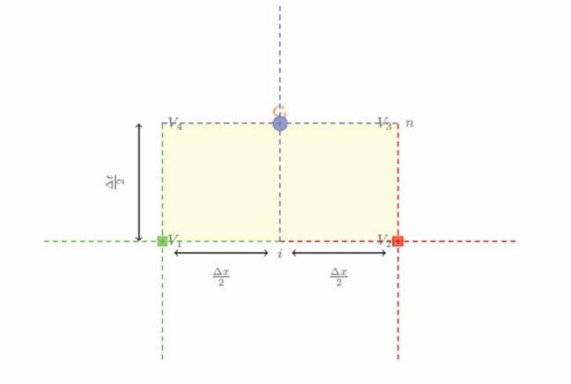


Fig. 2: Schemetic of i_{th}CE and its associated SEs.

2 shows, CE (C_i) is the polygon $V_1V_2V_3V_4$ and its corresponding SE is the union of dotted region. The solution point C_i and nodes V_3,V_4 are at the time level n while the nodes V_1,V_2 are t time level $(n-\frac{1}{2})$.
The whole domain is divided in a sense that all the conservation elements and solution elements possess following features:

1. All CEs are are non-overlapping and their union covers the space-time domain.
2. The SEs cover the boundaries of all the CEs but never overlap with each other.

The conservation law form of shallow water MHD equations holds for an arbitrary closed spacetime domain and the defined CE is also closed space-time region so the conservation law can be transformed to discrete form using this geometrical discretization. The boundaries of the CEs are parallel to the coordinate lines as well as the normal vectors are also along the coordinate axis. Hence only one component of space-time flux vector is left for integration over the boundary of CEs that makes the derivation of higher order scheme much more convenient. The conservation law is imposed on each CE and the spacetime flux is approximated by Taylor expansion within each SE. It is emphasized that the order of scheme results from the order of Taylor expansion for example the first-order Taylor expansion results the second-order scheme. Hence it is straightforward that the fourth-order scheme requires the third-order Taylor expansion. Moreover the CEs, SEs, and stencils possess the two properties (listed above) for the second and higher order scheme. Consider the i_{th} node as an example. By imposing Eq.5 on the i_{th} CE, I obtain

$$\int_{A(CE(C_i))} h_m \cdot ds = \int_{A(V_1V_2V_3V_4)} h_m \cdot ds = 0. \qquad (9)$$

The integration $\int_{A(V_1V_2V_3V_4V)} h_m \cdot ds$ in Eq.(7) involves integration over the bottom curve V_1V_2, integrating over the side curves V_1V_4, V_2V_3, and integration over the top curve V_4V_3. Let us integrate the spacetime fluxes over each part of i_{th} CE. The components of conserved variables and fluxes are u_m

and f_m where m = 1,2,...,5. The respective partial derivatives with respect to space variables x and time variable t are written as u_{mt},f_{mx}.

The dot product of flux vector and normal vector follows that only the spacetime flux U passes through the curve V_1V_2. I approximate u_m by the third-order Taylor expansion at the points V_1,V_2,V_3,V_4. using the discrete values $u_m(x_i,t^n)$ inside SE at each i_{th} node. In Fig.2, along the right part of dotted green horizontal line $u_m(x_i,t^n)$ is approximated by the third-order Taylor expansion at the point V_1

$$\int_{(i-\frac{1}{2})}^{i\Delta x} \{(u_m)_{v_1} + (u_{mx})_{v_1}\left[x-\left(i-\frac{1}{2}\right)\Delta x\right] + \frac{1}{2}(u_{mxx})_{v_1}\left[x-\left(i-\frac{1}{2}\right)\Delta x\right]^2 \quad (10)$$

(11)

(12)

$$+\frac{1}{6}(u_{mxxx})_{v_1}\left[x-\left(i-\frac{1}{2}\right)\Delta x\right]^3\} \quad (13)$$

$$=\frac{\Delta x}{2}\{(u_m)_{v_1} + (u_{mx})_{v_1}\frac{\Delta x}{4} + + (u_{mxx})_{v_1}\frac{\Delta x^2}{24} \quad (14)$$

$$+(u_{mxxx})_{V_1}\frac{\Delta x^3}{192}\}. \quad (15)$$

(16)

Similarly, along the left part of dotted red horizontal line $u_m(x_i,t^n)$ is approximated by the third-order Taylor expansion at the point V_2

$$\int_{i\Delta x}^{(i+\frac{1}{2})} \{(u_m)_{v_2} + (u_{mx})_{v_2}\left[x-\left(i+\frac{1}{2}\right)\Delta x\right] + \frac{1}{2}(u_{mxx})_{v_2}\left[x-\left(i+\frac{1}{2}\right)\Delta x\right]^2 \quad (17)$$

(18)

(19)

$$+\frac{1}{6}(u_{mxxx})_{v_2}\left[x-\left(i+\frac{1}{2}\right)\Delta x\right]^3\} \quad (20)$$

$$=\frac{\Delta x}{2}\{(u_m)_{v_2} - (u_{mx})_{v_2}\frac{\Delta x}{4} + (u_{mxx})_{v_2}\frac{\Delta x^2}{24} \quad (21)$$

$$-(u_{mxxx})_{V_2}\frac{\Delta x^3}{192}\}. \quad (22)$$

(23)

The space-time flux f is the only the component that passes through the side faces V_1V_4 and V_2V_3 of CE in the direction of the t axis. Again using the third-order Taylor expansion at the points V_1 and V_2. gives the following results:

$$\int_{(n-\frac{1}{2})\Delta t}^{n\Delta t} \{(f_m)_{v_1} + (f_{mt})_{v_1}\left[t-\left(n-\frac{1}{2}\right)\Delta t\right] + \frac{1}{2}(f_{mtt})_{v_1}\left[t-\left(n-\frac{1}{2}\right)\Delta x\right]^2 \quad (24)$$

(25)

$$+\frac{1}{6}(f_{mttt})_{v_1}\left[t-\left(i-\frac{1}{2}\right)\Delta x\right]^3\} \quad (26)$$

(27)

$$=\frac{\Delta t}{2}\{(f_m)_{v_1} + (f_{mt})_{v_1}\frac{\Delta t}{4} + + (f_{mtt})_{v_1}\frac{\Delta t^2}{24} + (f_{mttt})_{V_1}\frac{\Delta t^3}{192}\} \quad (28)$$

(29)

and

$$\int_{n\Delta t}^{(n+\frac{1}{2})\Delta t} \{(f_m)_{v_2} + (f_{mt})_{v_2}\left[t-\left(n+\frac{1}{2}\right)\Delta t\right] + \frac{1}{2}(f_{mtt})_{v_2}\left[t-\left(n+\frac{1}{2}\right)\Delta x\right]^2 \quad (30)$$

(31)

(32)

$$+\frac{1}{6}(f_{mttt})_{v_2}\left[t-\left(i+\frac{1}{2}\right)\Delta x\right]^3\} \quad (33)$$

$$=\frac{\Delta t}{2}\{(f_m)_{v_2} - (f_{mt})_{v_2}\frac{\Delta t}{4} + + (f_{mtt})_{v_2}\frac{\Delta t^2}{24} + (f_{mttt})_{V_2}\frac{\Delta t^3}{192}\} \quad (34)$$

(35)

Integration along the curve V_3V_4 gives

$$\int_{(i-\frac{1}{2})\Delta x}^{(i+\frac{1}{2})i\Delta x} \{(u_m)_{C_i} + (u_{mx})_{C_i}[x-i\Delta x] + \frac{1}{2}(u_{mxx})_{C_i}[x-i\Delta x]^2 + \frac{1}{6}(u_{mxxx})_{C_i}[x-i\Delta x]^3\} \quad (36)$$

(37)

$$=\frac{\Delta x}{2}\{(u_m)_{C_i} + (u_{mxx})_{C_i}\frac{\Delta x^2}{24}\} \quad (38)$$

(39)

(40)

Integration over the all the boundary curves of CE at the i_{th} node gives updated values of conserved variables at n_{th} time level in terms of the values at $(n-\frac{1}{2})$ time level as follows:

$$\text{umupdated} = \left(I_{\text{bottom}} - \text{XI side} - I_{\text{top}}\right)/\Delta x, \quad (41)$$

where I stands for the integration over bottom, sides and top

curves of CE. Finally, this process allows to write

$$(u_m)_i^n = \frac{1}{\Delta x}\sum_{l=1}^{2}\{\frac{\Delta x}{2}\{(u_m)_l^{n-1/2} + (u_{mx})_l^{n-1/2}\left(k_x\frac{\Delta x}{4}\right) \quad (42)$$

$$+\frac{1}{24}(u_{mxx})_l^{n-1/2}(k_x\Delta x)^2 + \frac{1}{192}(u_{mxxx})_l^{n-1/2}(k_x\Delta x)^3\} \quad (43)$$

$$+k_x\frac{\Delta t}{2}\{(f_m)_l^{n-\frac{1}{2}} + (f_{mt})_l^{n-1/2}\frac{\Delta t}{4} \quad (44)$$

$$+(f_{mtt})_l^{n-1/2}(\Delta t)^2\frac{1}{24} + \frac{1}{192}(f_{mttt})_l^{n-1/2}(\Delta t)^3\}\rangle \quad (45)$$

$$-\frac{1}{24}(u_{mxx})_j^{n-\frac{1}{2}}. \quad (46)$$

Here l is the subscript that represent solution points V_1 and V_2 and k_x is 1 for V_2 and -1 for V_1.

A. Higher order derivatives of flux function f_m

The space and time derivatives fmx, fmxx, fmxxx, fmt, fmtt and fmttt etc are obtained according to the chain rule. The first order derivatives are given as

$$\frac{\partial f_m}{\partial x} = \sum_{r=1}^{5} \frac{\partial f_m}{\partial u_r} \frac{\partial u_r}{\partial x}, \quad (47)$$

and

$$\frac{\partial f_m}{\partial t} = \sum_{r=1}^{5} \frac{\partial f_m}{\partial u_r} \frac{\partial u_r}{\partial t}. \quad (48)$$

Again applying the chain rule to first order derivatives results the following second order flux component's derivatives:

$$\frac{\partial^2 f_m}{\partial x^2} = \sum_{r=1}^{5} \frac{\partial f_m}{\partial u_r} \frac{\partial^2 u_r}{\partial x^2} + \sum_{r=1}^{5}\sum_{s=1}^{5} \frac{\partial^2 f_m}{\partial u_r \partial u_s} \frac{\partial u_r}{\partial x} \frac{\partial u_s}{\partial x}, \quad (49)$$

$$\frac{\partial^2 f_m}{\partial x \partial t} = \sum_{r=1}^{5} \frac{\partial f_m}{\partial u_r} \frac{\partial^2 u_r}{\partial x \partial t} + \sum_{r=1}^{5}\sum_{s=1}^{5} \frac{\partial^2 f_m}{\partial u_r \partial u_s} \frac{\partial u_r}{\partial x} \frac{\partial u_s}{\partial t}, \quad (50)$$

and

$$\frac{\partial^2 f_m}{\partial t^2} = \sum_{r=1}^{5} \frac{\partial f_m}{\partial u_r} \frac{\partial^2 u_r}{\partial t^2} + \sum_{r=1}^{5}\sum_{s=1}^{5} \frac{\partial^2 f_m}{\partial u_r \partial u_s} \frac{\partial u_r}{\partial t} \frac{\partial u_s}{\partial t}. \quad (51)$$

Similarly the third-order derivatives can be calculated using the chain rule. The third order derivatives are given below.

$$\frac{\partial^2 f_m}{\partial t^2} = \sum_{r=1}^{5} \frac{\partial f_m}{\partial u_r} \frac{\partial^2 u_r}{\partial t^2} + \sum_{r=1}^{5}\sum_{s=1}^{5} \frac{\partial^2 f_m}{\partial u_r \partial u_s} \frac{\partial u_r}{\partial t} \frac{\partial u_s}{\partial t}. \quad (51)$$

$$f_{mxxx} = \sum_{p=1}^{5} \frac{\partial f_m}{\partial u_p} . u_{pxxx} + \sum_{p=1}^{5}\sum_{q=1}^{5} \frac{\partial^2 f_m}{\partial u_p \partial u_q} \left(u_{pxx} . u_{qx} + u_{qxx} u_{px}\right) \quad (52)$$

(53)

$$+ \sum_{p=1}^{8}\sum_{q=1}^{8}\sum_{r=1}^{5} \frac{\partial^3 f_m}{\partial u_p \partial u_q \partial u_r} u_{px} . u_{qx} . u_{rx}, \quad (54)$$

$$f_{mxxt} = \sum_{p=1}^{5} \frac{\partial f_m}{\partial u_p} . u_{pxxt} \quad (55)$$

$$+ \sum_{p=1}^{5}\sum_{q=1}^{5} \frac{\partial^2 f_m}{\partial u_p \partial u_q} \left(u_{pxx} . u_{qt} + u_{pxt} . u_{qx} + u_{pxt} u_{qx}\right) \quad (56)$$

$$+ \sum_{p=1}^{8}\sum_{q=1}^{8}\sum_{r=1}^{5} \frac{\partial^3 f_m}{\partial u_p \partial u_q \partial u_r} u_{px} . u_{qx} . u_{rt}, \quad (57)$$

$$f_{mxtt} = \sum_{p=1}^{5} \frac{\partial f_m}{\partial u_p} . u_{pxtt} \quad (58)$$

$$+ \sum_{p=1}^{5}\sum_{q=1}^{5} \frac{\partial^2 f_m}{\partial u_p \partial u_q} \left(u_{pxt} . u_{qt} + u_{ptt} . u_{qx} + u_{pxt} u_{qt}\right) \quad (59)$$

$$+ \sum_{p=1}^{8}\sum_{q=1}^{8}\sum_{r=1}^{5} \frac{\partial^3 f_m}{\partial u_p \partial u_q \partial u_r} u_{px} . u_{qt} . u_{rt}, \quad (60)$$

and

$$f_{mttt} = \sum_{p=1}^{5} \frac{\partial f_m}{\partial u_p} . u_{pttt} + \sum_{p=1}^{5}\sum_{q=1}^{5} \frac{\partial^2 f_m}{\partial u_p \partial u_q} \left(u_{ptt} . u_{qt} + u_{ptt} . u_{qt} + u_{ptt} u_{qt}\right) \quad (61)$$

(62)

$$+ \sum_{p=1}^{8}\sum_{q=1}^{8}\sum_{r=1}^{5} \frac{\partial^3 f_m}{\partial u_p \partial u_q \partial u_r} u_{pt} . u_{qt} . u_{rt}. \quad (63)$$

The derivatives of flux components $\frac{\partial f_m}{\partial u_p}$, $\frac{\partial^2 f_m}{\partial u_p \partial u_g}$ and $\frac{\partial^3 T_m}{\partial u_p \partial u_g \partial u_r}$ are entries of the Jacobian matrices. For shallow water MHD equations, these derivatives are obtained by Matlab symbolic computations specially for the third order case. The computation of time derivatives of flux variables are obtained by using the conservation law.

$u_{mt} = -f_{mx}$. (64)

Taking derivative with respect to space variable x on both sides and treating the mixed space and time derivatives same allows to write down

$$umxt = -fmxx. \quad (65)$$

Similarly, for time variable t

$$umtt = -fmxt. \quad (66)$$

Getting these derivatives and using the equations 48,49,50 and 51 provides the values of f_{mt},f_{mxt} and f_{mtt}. Again taking the time and space derivatives on both sides of equation 66 follows

$$\text{and} \quad umxtt = -fmxxt, \quad (67)$$

$$umttt = -fmxtt. \quad (68)$$

Using 67 and 68 gives f_{mttt}.

B. Spatial Derivatives of Conserved Variables

At this point, all the time derivatives of conservative variables are available through the derivatives of flux f_m and the flux derivatives. Now at the end it is only left to get the space derivative variables of u_m such as u_mx,u_my,u_{mxx}, and u_{mxxx}. The first derivative u_mx is updated at the i_th node using the updated values of u_m obtained from Equation 64. In general each higher order space derivatives of conserved variables is updated using the updated values of next higher order derivative. Now, for the fourth-order scheme, the values of two more derivatives $u_m$xx and $u_m$xxx are required to update.Proceeding in following steps allows to get the updated values of all derivatives:

1: updating u_{mxxx} at C_i;

2: updating u_{mxx} at C_i; 3: updating u_m at C_i; 4: updating u_{mx} at C_i.

This process has been adopted from the work of Shen et al. [14] with slight modification due to one-dimensional problem. Expand u_{mxx} in Taylor expension at V_3 and V_4, it

gives

$$\text{umxx(V4)} = \text{umxx(Ci)} + \text{umxxx(Ci)}\Delta\text{xV4Ci}, \quad (69)$$

and

$$\text{umxx(V3)} = \text{umxx(Ci)} + \text{umxxx(Ci)}\Delta\text{xV3Ci}, \quad (70)$$

The values at V_3 and V_4 are approximated using the Taylor expansion in time at these nodes. Subtracting these two equations gives:

$$u_{mxxx}(C_i) = \frac{[u_{mxx}(V_4) - u_{mxx}(V_3)]}{\Delta x_{C_iV_4} - \Delta x_{C_iV_3}}, \quad (71)$$

where

$$u_{mxx}(V_4) = u_{mxx}(V_1) + u_{mxxx}(V_1)\frac{\Delta t}{2}, \quad (72)$$

and

$$u_{mxx}(V_3) = u_{mxx}(V_2) + u_{mxxx}(V_2)\frac{\Delta t}{2}. \quad (73)$$

Similarly, the second order derivative u_{mxx} is obtained at n_{th} time level in terms of the values at $n-\frac{1}{2}$ time level and is given by.

$$u_{mxx}(C_i) = \frac{[u_{mx}(V_4) - u_{mx}(V_3)]}{\Delta x_{C_iV_4} - \Delta x_{C_iV_3}}, \quad (74)$$

where

$$u_{mx}(V_4) = u_{mx}(V_1) + u_{mxx}(V_1)\frac{\Delta t}{2}, \quad (75)$$

and

$$u_{mx}(V_3) = u_{mx}(V_2) + u_{mxx}(V_2)\frac{\Delta t}{2}, \quad (76)$$

where ΔxCiV3 = xCi − xV3 and ΔxCiV4 = xCi − xV4.

C. Time Marching the First-order Derivative

The first-order derivative u_{mx} is approximated via same process and using the third-order Taylor series expansion at points V_3 and V_4. It gives

$$u_m(V_3) = u_m(C_i) + u_{mx}(C_i)\Delta x_{V_3C_i} + \frac{1}{2}\left[u_{mxx}(C_i)\right(+ \frac{1}{6}\left[u_{mxxx}(C_i)\left(\Delta x_{C_iV_3}\right)^3\right], \quad (77)$$

and

$$u_m(V_4) = u_m(C_i) + u_{mx}(C_i)\Delta x_{V_4C_i} + \frac{1}{2}\left[u_{mxx}(C_i)\right(+ \frac{1}{6}\left[u_{mxxx}(C_i)\left(\Delta x_{C_iV_4}\right)^3\right], \quad (78)$$

In equations 78 and 77, the values $u_m(V_3)$ and $u_m(V_4)$ are obtained from the Taylor expansion in time variable at n_{th} time level.

$$u_m(V_3') = u_m(V_2) + u_{mt}(V_2)\frac{\Delta t}{2} + \frac{1}{2}u_{mtt}(V_2)\left(\frac{\Delta t}{2}\right)^2 + \frac{1}{6}u_{mttt}(V_2)\left(\frac{\Delta t}{2}\right)^3,$$

and

$$u_m(V_4') = u_m(V_1) + u_{mt}(V_1)\frac{\Delta t}{2} + \frac{1}{2}u_{mtt}(V_1)\left(\frac{\Delta t}{2}\right)^2 + \frac{1}{6}u_{mttt}(V_1)\left(\frac{\Delta t}{2}\right)^3.$$

The weighted average is employed in order to reduce numerical oscillations. Finally the first-order derivatives are approximated below as:

$$u_{mx}(C_i) = u_m(V_3, V_4; \alpha) = \frac{|u(V_3)|^\alpha u(V_4) + |u(V_3)|^\alpha u(V_4)}{|u(V_3)|^\alpha + |u(V_4)|^\alpha} \quad (79)$$

.

where α is the adjusting parameter taken as 1, 1.5 or 2.

III. THE RIEMANN PROBLEM SIMULATION

A numerical test is performed to demonstrate the robustness and the accuracy of 4th-order CESE scheme over 2ndorder CESE schem. A strong Riemann problem has been solved here. This problem is taken from [17]. The initial conditions are given as:

$$\begin{bmatrix} h \\ v_1 \\ v_2 \\ B_1 \\ B_2 \end{bmatrix} = \begin{cases} [1,0,0,1,0]^T, & \text{if } x \le 0 \\ [2,0,0,0.5,1]^T & \text{if } x > 0 \end{cases} \quad (80)$$

The problem is solved with periodic boundary conditions and domain Ω = [−1,1] at t = 0.4. The results are shown in Figures 3-7. As expected, it is clear seen that the fourth-order scheme shows remarkable details in the solution compared to the second -order scheme at same grid of 1000 nodes. Moreover it is observed that the fourth-order scheme advantages over the second order scheme by showing much better results even with less grid. Indeed, the results conclude that the fourth order scheme is computationally more efficient and also accurate.

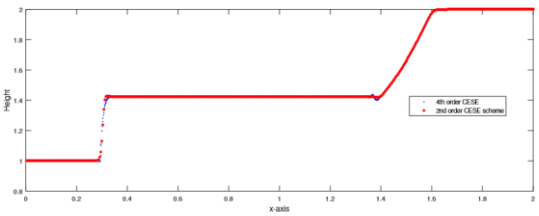


Fig. 3: Height at t = 0.4

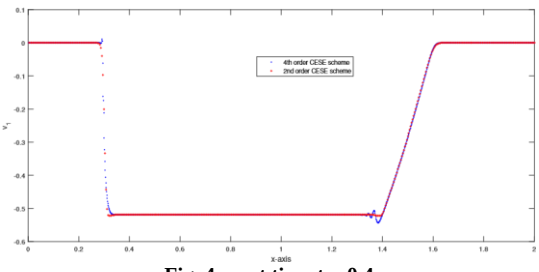


Fig. 4: v_1 at time t = 0.4

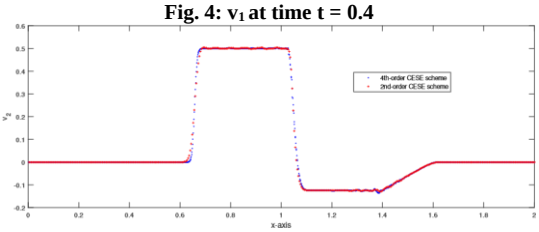


Fig. 5: v_2 at time t = 0.2

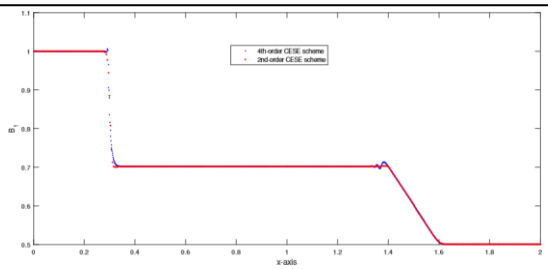


Fig. 6: B_1 at time t = 0.4

CONCLUSIONS

The fourth-order CESE method is presented in detail for SWMHD equations. The benchmark test revealed excellent characteristics of the method. The scheme is based on unified treatment of space and time variables that allows a systematic and easy extension to higher dimensions as well as to arbitrary higher order scheme. The scheme is computationally efficient and accurate and outperforms tha second-order CESE method even with less grid. The divergence constraint is automatically satisfied for the one-dimensional SWMHD system. Hence the discussion is restricted to only CESE method formulation.

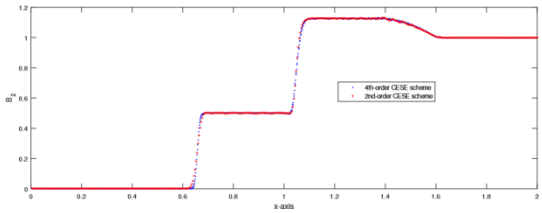


Fig. 7: B_2 at time t = 0.4

This work can be extended to higher dimensional SWMHD system that I will present in near future.

Funding: This work has been carried out as a part of project under the grant by Higher Education Commission of Pakistan vide office letter No. HEC/FD/2017/4325. I also acknowledge Sukkur IBA University for providing state of the art research environment.

REFERENCES

[1] Balsara, Dinshaw S., Michael Dumbser, and Remi Abgrall. ”Multidimensional HLLC Riemann solver for unstructured mesheswith application to Euler and MHD flows.” Journal of Computational Physics 261 (2014): 172-208.

[2] CHANG, Sin-Chung, Sheng-Tao YU, Ananda HIMANSU, Xiao-Yen WANG, Chuen-Yen CHOW, and Ching-Yuen LOH. ”The method of space-time conservation element and solution elementA new paradigm for numerical solution of conservation laws.” In Computational Fluid Dynamics Review 1998: (In 2 Volumes), pp. 206-240. 1998. Application of spacetime CE/SE method to shallow water magnetohydrodynamic equations.” Journal of computational and applied mathematics 196, no. 1 (2006): 132-149.

[3] De Sterck, Hans. ”Hyperbolic theory of the shallow water magnetohydrodynamics equations.” Physics of plasmas 8, no. 7 (2001): 3293-3304.

[4] Dikpati, Mausumi, and Peter A. Gilman. ”Flux-transport dynamos with α - effect from global instability of tachocline differential rotation: a solution for magnetic parity selection in the Sun.” The Astrophysical Journal 559, no. 1 (2001): 428.

[5] Dikpati, Mausumi, and Peter A. Gilman. ”Prolateness of the solar tachocline inferred from latitudinal force balance in a magnetohydrodynamic shallow-water model.” The Astrophysical Journal 552, no. 1 (2001): 348.

[6] Fuchs, Franz Georg, Andrew D. McMurry, Siddhartha Mishra, Nils Henrik Risebro, and Knut Waagan. ”Approximate Riemann solvers and robust high-order finite volume schemes for multi-dimensional ideal MHD equations.” Communications in Computational Physics 9, no. 2 (2011): 324-362.

[7] Gilman, Peter A. ”Magnetohydrodynamic shallow water equations for the solar tachocline.” The Astrophysical Journal Letters 544, no. 1 (2000): L79.

[8] Jiang, Chaowei, Xueshang Feng, Jian Zhang, and Dingkun Zhong. ”AMR simulations of magnetohydrodynamic problems by the CESE method in curvilinear coordinates.” Solar Physics267, no. 2 (2010): 463491.

[9] Krger, Tim, and Mria Lukov-Medvidov. ”An evolution Galerkin scheme for the shallow water magnetohydrodynamic equations in two space dimensions.” Journal of Computational Physics 206, no. 1 (2005): 122149.

[10] Massimi, H. Saldivar, H. Shen, and C. Y. Wen. ”Study of Hypersonic Dissociating Flows over Spheres Using the Space-Time CE/SE Method.” In 30th International Symposium on Shock Waves 1, pp. 145-148. Springer, Cham, 2017.

[11] Qamar, Shamsul, and Sidrah Mudasser. ”On the application of a variant CE/SE method for solving two-dimensional ideal MHD equations.” Applied numerical mathematics 60, no. 6 (2010): 587-606.

[12] Qamar, Shamsul, and Gerald Warnecke. ”Application of spacetime CE/SE method to shallow water magnetohydrodynamic equations.” Journal of computational and applied mathematics 196, no. 1 (2006): 132149.

[13] Rossmanith, James Alexander. A wave propagation method with constrained transport for ideal and shallow water magnetohydrodynamics. 2002.

[14] Rossmanith, James A. ”A constrained transport method for the shallow water MHD equations.” In Hyperbolic Problems: Theory, Numerics, Applications, pp. 851-860. Springer, Berlin, Heidelberg, 2003.

[15] Shen, Hua, and Matteo Parsani. ”Positivity-preserving CE/SE schemes for solving the compressible Euler and NavierStokes equations on hybrid unstructured meshes.” Computer Physics Communications 232 (2018): 165-176.

[16] Wang, Gang, Deliang Zhang, Kaixin Liu, and Jingtao Wang. ”An improved CE/SE scheme for numerical simulation of gaseous and twophase detonations.” Computers and Fluids 39, no. 1 (2010): 168-177.

[17] Winters, Andrew R., and Gregor J. Gassner. ”An entropy stable finite volume scheme for the equations of shallow water magnetohydrodynamics.” Journal of Scientific Computing 67, no. 2 (2016): 514-539.

[18] Yang, Yun, Xue-Shang Feng, and Chao-Wei Jiang. ”A high-order CESE scheme with a new divergence-free method for MHD numerical simulation.” Journal of Computational Physics 349 (2017): 561-581.

[19] Yu, Sheng-Tao John, Lixiang Yang, Robert L. Lowe, and Stephen E. Bechtel. ”Numerical simulation of linear and nonlinear waves in hypoelastic solids by the CESE method.” Wave Motion 47, no. 3 (2010): 168-182.

★★★